Magnetic Resonance in Medicine 64:1472–1478 (2010)

Quantitative Assessment of Left Ventricular Function in Humans at 7 T

Anne Brandts, Jos J. M. Westenberg,* Maarten J. Versluis, Lucia J. M. Kroft, Nadine B. Smith, Andrew G. Webb, and Albert de Roos

The purpose of this study was to determine the ability of 7 T cardiac magnetic resonance imaging (MRI) to quantitatively assess left ventricular volumes, mass, and function from cine short-axis series and left ventricular diastolic filling from velocity-encoded MRI in 10 healthy volunteers. As comparative "gold standard," the corresponding measures obtained at 1.5 T were taken. Left ventricular volumes, function, and mass were obtained by manual image segmentation. Trans-mitral flow graphs were obtained from 2D one-directional through-plane velocity-encoded MRI planned at the mitral valve in end-systole. Imaging at 7 T MRI was successful in 80% of the examinations. Assessment of left ventricular volumes, function, and mass at 7 T showed good agreement with 1.5 T (no significant differences between variables describing volumes, function, and mass with intraclass correlation coefficients ranging from 0.77 to 0.96). Trans-mitral stroke volume and the ratio between early and atrial peak filling rate showed strong agreement at both field strengths (no significant differences between stroke volumes and filling ratios with intraclass correlation coefficients 0.92 for stroke volumes and 0.77 for peak filling ratios). In conclusion, this study shows that assessing left ventricular volumes, function, and flow is feasible at 7 T MRI and that standardized MRI protocols provide similar quantitative results when compared with 1.5 T MRI. Magn Reson Med 64:1472–1478, 2010. © 2010 Wiley-Liss, Inc.

Key words: 7 Tesla MRI; cardiac magnetic resonance imaging; velocity-encoding; left ventricular function

INTRODUCTION

High-field in vivo visualization of the human heart (1,2) and coronary arteries (3) has recently been shown using human whole-body 7 T MRI systems. There are many potential challenges from the increased field strength, including decreased T_2^*-times, increased B_0 inhomogeneities, nonuniform sample-induced B_1-distributions, and significantly increased radiofrequency (RF) deposition. Specific to cardiac imaging, both the conservative constraints regarding the specific absorption rate (SAR) and the increased B_0 inhomogeneities have so far prevented the use of steady-state free-precession (SSFP) sequences, which are much more efficient than simple gradient-echo alternatives. In addition, the increased magneto-hydrodynamic disturbance of the electrocardiographic (ECG)-signal presents considerable challenges for efficient data acquisition (4). Finally, there is limited availability of optimized RF hardware in terms of a body transmit coil.

Feasibility for cardiac MRI at a human whole-body 7 T MRI system was demonstrated by Snyder et al. (1). Using an eight-channel transmit/receive array coil and local B_1 shimming, they were able to obtain breath-hold anatomical and functional short-axis and four-chamber vector ECG-gated cine segmented gradient-echo series in volunteers. Similar results have been reported by other groups (5,6). However, despite the impressive image quality, no quantitative information was obtained, nor was comparison with SSFP performed in a head-to-head comparison with cardiac MRI at 1.5 T which is the accepted reference standard in cardiac MRI. Furthermore, diastolic left ventricular (LV) filling using velocity-encoded (VE) MRI has not previously been studied at 7 T MRI. Therefore, the purpose of the current study was to quantitatively compare assessment of LV volumes, mass and systolic function, and image quality from multislice short-axis cine MRI as well as LV diastolic filling from VE MRI in 10 healthy volunteers in a comparison between 7 T MRI and 1.5 T MRI.

MATERIALS AND METHODS

Both 1.5 T MRI and 7 T MRI protocols were approved by the local medical ethics committee and all volunteers gave written informed consent. Ten healthy volunteers (mean age 28 ± 9 years, seven male) without any history of cardiovascular disease were recruited. Subjects underwent MRI examinations on the 1.5 T MRI and 7 T MRI systems on the same day.

7 T MRI

A commercial human whole-body 7 T MRI system (Philips Achieva, Philips Medical Systems, Best, The Netherlands) equipped with a vector-ECG-gating setup (7) and a custom-built 13-cm-diameter quadrature double-loop RF transmit/receive surface coil operating at 298.1 MHz was used. RF pulses were calibrated using the manufacturer provided method that uses the ratio between a spin echo and a stimulated echo to calculate the flip angle (8,9). The inhomogeneous excitation pattern of the RF coil results in a much reduced flip angle in the myocardium compared with regions closer to the coil. The flip angles used for the experiments in this study were empirically optimized to give optimal contrast or signal. The setup has been described in detail previously (3). All subjects were positioned head first in the scanner in a supine position with the position of the heart at the magnet iso-center. A 1-cm gap was introduced between the RF coil and the anterior chest wall of the subject using a foam rubber

Department of Radiology, Leiden University Medical Center, Leiden, The Netherlands.

*Correspondence to: Jos J. M. Westenberg, PhD, Department of Radiology, Leiden University Medical Center, Albinusdreef 2, 2333 ZA Leiden, The Netherlands. E-mail: j.j.m.westenberg@lumc.nl

Received 2 March 2010; revised 4 May 2010; accepted 17 May 2010.

DOI 10.1002/mrm.22529

Published online 30 June 2010 in Wiley Online Library (wileyonlinelibrary.com).

spacer to reduce patient-induced losses (10). Triggering off the R-wave of the vector-ECG recording was feasible despite the significantly amplified and broadened signal of the T-wave due to the magneto-hydrodynamic effect.

First, nontriggered multistack multitwo-dimensional (2D) segmented gradient-echo series in coronal, sagittal, and axial orientations were obtained during free breathing to produce a complete survey of the thorax. Next, based on the survey images, LV and right ventricular (RV) two-chamber and four-chamber RF spoiled segmented *k*-space gradient echo sequences were obtained using retrospective gating within single 12–15 sec breath-holds: echo time (TE) 2.2 msec, repetition time (TR) 4 msec, flip angle (α) 15°, slice thickness 8 mm, field-of-view (FOV) 380 × 247 mm^2, scan matrix 292 × 269 retrospectively reconstructed in 33 phases for one cardiac cycle with 432 × 432 image resolution, and reconstructed pixel size 0.88 × 0.88 mm^2, number of signal averages (NSAs) 1. The multislice multiphase cine gradient-echo short-axis series were obtained with one slice per breath-hold: TE 1.7 msec, TR 4 msec, α 15°, slice thickness 10 mm, 10–12 consecutive slices without gap, FOV 380 × 247 mm^2 scan matrix 292 × 273, retrospectively reconstructed in 33 phases for one cardiac cycle with 432 × 432 image resolution and pixel size 0.88 × 0.88 mm^2, NSA 1. Trans-mitral flow was obtained from 2D one-directional through-plane VE MRI with velocity sensitivity of 150 cm/sec: TE 2.6 msec, TR 4.6 msec, α 20°, slice thickness 8 mm, FOV 350 × 228 mm^2, scan matrix 128 × 73, retrospectively reconstructed in 40 phases for one cycle with 240 × 240 image resolution and a reconstructed pixel size 1.5 × 1.5 mm^2, and an acquired pixel size of 2.73 × 3.12 mm^2, NSA 2, positioned at the location of the mitral valve at the end-systolic moment in both LV two-chamber and four-chamber views, and perpendicular to the inflow direction.

1.5 T MRI

A commercial human whole-body 1.5 T MRI system (ACS-NT15 Intera, Philips Medical Systems, Best, The Netherlands; software release 12, Pulsar gradient system with amplitude 33 mT/m and 100 mT/(m msec) slew rate, 0.33 msec rise time) with vector-ECG gating, body transmit, and a five-element cardiac receive coil was used for comparison studies. A similar imaging protocol as at 7 T MRI was followed. Also for these studies, first a nontriggered multistack multi-2D segmented gradient-echo coronal, sagittal, and axial survey of thorax was obtained. LV and RV two-chamber and four-chamber segmented cine SSFP gradient-echo series with retrospective gating were obtained within single 8–10 sec breath-holds: TE 1.5 msec, TR 3 msec, α 50°, slice thickness 10 mm, FOV 400 × 320 mm^2, scan matrix 208 × 161, retrospectively reconstructed in 30 phases for one cardiac cycle with 256 × 256 image resolution and pixel size 1.6 × 1.6 mm^2, NSA 1. The multislice multiphase cine SSFP gradient-echo short-axis series were obtained with one slice per breath-hold, without the use of parallel imaging: TE 1.7 msec, TR 3.5 msec, α 35°, slice thickness 10 mm, 10–12 consecutive slices without gap, FOV 450 × 360 mm^2, scan matrix 256 × 193, retrospectively reconstructed in 40 phases for one cardiac cycle with 256 × 256 image resolution and pixel size 1.8 × 1.8 mm^2, NSA 1. Two-dimensional one-directional through-plane VE MRI with velocity sensitivity of 150 cm/sec was performed for trans-mitral flow assessment: TE 5.8 msec, TR 9 msec, α 20°, slice thickness 8 mm, FOV 350 × 280 mm^2, scan matrix 128 × 102, retrospectively reconstructed in 40 phases for one cycle with 256 × 256 image resolution and a reconstructed of pixel size 1.4 × 1.4 mm^2, acquired pixel size 2.73 × 2.74 mm^2, NSA 2.

Image Processing

LV volumes, function, and mass were obtained by manual image segmentation using the in-house developed analytical software program MASS (Leiden University Medical Center, Leiden, The Netherlands) (11). LV volume assessment by short-axis planimetry has been extensively validated and widely applied in clinical research (12). Phases of end-diastole (ED) and end-systole (ES) were visually determined in the mid-ventricular slice. LV endocardial and epicardial contours were manually segmented in ED and ES. Papillary muscles were considered to be part of the LV cavity. Left ventricular end-diastolic volume and left ventricular end-systolic volume were obtained by endocardial area assessment and summation of discs, stroke volume was obtained by subtraction of left ventricular end-diastolic volume-left ventricular end-systolic volume, LV ejection fraction was calculated by the ratio between stroke volume and left ventricular end-diastolic volume, and finally LVED mass (LVEDM) was determined by subtraction of endocardial segmented volume from epicardial segmented volume multiplied by the myocardial mass density (1.05 g/mL).

Trans-mitral flow graphs were obtained by manual contour segmentation performed using the in-house developed software program FLOW (Leiden University Medical Center, Leiden, The Netherlands) (13). Background correction was performed (mandatory for both correction for local phase offset errors (14) as well as correction for through-plane motion as suggested by Kayser et al. (15)) from the velocity of the myocardium in the lateral wall near the mitral inflow region. Trans-mitral stroke volume as well as early peak filling rate, atrial peak filling rate, and E/A-ratio were determined from the trans-mitral flow graphs.

In both 7 T MRI and 1.5 T MRI-acquired cine short-axis data sets, signal-to-noise ratio (SNR) and contrast-to-noise ratio were determined in the ED-phase in a mid-ventricular slice. SNR was calculated in the interventricular septum, in LV lateral wall, and in the LV blood pool, by obtaining the average signal measured in circular sampling regions-of-interests (ROIs) of 1 cm^2 positioned in the middle of the interventricular septum, in the middle of the LV lateral wall, and in the center of the LV blood pool, respectively, and the standard deviation of the noise, obtained from a similar 1 cm^2 regions-of-interest positioned in an artifact-free area well outside the body. Also, the contrast-to-noise ratio between LV blood pool and interventricular septum (= SNR blood pool – SNR septum) and between LV blood pool and LV lateral wall (= SNR blood pool – SNR lateral wall) was determined.

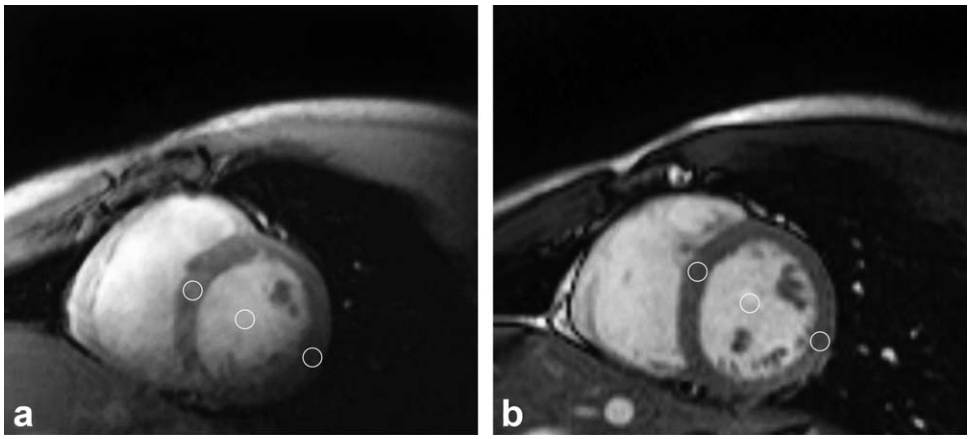

FIG. 1. Example of a mid-ventricular end-diastolic short-axis image of the same volunteer at 7 T using an RF-spoiled gradient echo sequence (**a**) and at 1.5 T using a balanced steady state gradient echo sequence (**b**). Region-of-interests (ROIs) indicate the locations for signal analysis: in the interventricular septum, in the left ventricular lateral wall, and in the center of the left ventricular blood pool. Noise is measured in an artifact-free ROI in the air well outside the thorax.

A single observer with 3 years of experience in cardiac MR imaging performed all image analysis (A.B.), under supervision of a senior researcher with 15 years of experience in cardiac MR imaging (J.J.M.W.). Image analysis of 7 T MRI data was performed blinded with respect to the results obtained at 1.5 T MRI.

Statistical Analysis

Continuous variables are expressed as mean ± standard deviation. Correlation between results obtained at 7 T MRI and 1.5 T MRI were tested with intraclass correlation for absolute agreement. Mean differences between measurements were determined and their statistical significance was tested using paired *t*-tests. A *P*-value < 0.05 was considered statistically significant. Also, 95% confidence intervals as well as coefficients of variance (defined as the standard deviation of the differences between the two series of measurements divided by the mean of both measurements) were determined. The approach described by Bland and Altman (16) was followed to study systematic differences.

RESULTS

Imaging at 7 T MRI was successful in 8 of 10 volunteers (80%). Image quality was inadequate in two 7 T MRI studies due to ECG-triggering problems: these studies were excluded from further analysis. All volunteers tolerated both MRI examinations very well and breath-holding was equally successful. Volunteers did not report specific sensations during either examination. In Fig. 1, a representative example of the eight remaining studies is presented, showing both 7 T MRI (A) and corresponding 1.5 T MRI (B) mid-ventricular ED short-axis images. As expected, the spatial distribution of signal intensity is more homogeneous for the 1.5 T MR image due to the difference in coil arrangements.

LV Volumes, Function, and Mass

Table 1 shows LV volumes, function, and mass for 7 T MRI and 1.5 T. There were no statistically significant

Table 1
Comparison of Quantitative Results 7 T MRI Versus 1.5 T MRI

	7 T MRI, mean ± SD	1.5 T MRI, mean ± SD	mean difference ± SD	*P*-value	ICC (*P*-value)	95% CI	COV
LVEDV	148 ± 18 mL	156 ± 31 mL	−8 ± 21 mL	0.30	0.78 (0.03)	−23–8 mL	14%
LVESV	67 ± 11 mL	73 ± 20 mL	−6 ± 13 mL	0.20	0.77 (0.03)	−16–3 mL	19%
LV SV	81 ± 12 mL	83 ± 16 mL	−2 ± 12 mL	0.64	0.82 (0.03)	−10–6 mL	14%
LV EF	55 ± 5%	53 ± 7%	1 ± 4%	0.39	0.84 (0.02)	−2–4%	8%
LVEDM	111 ± 18 g	112 ± 21 g	−1 ± 8 g	0.66	0.96 (<0.001)	−7–4 g	7%
MV SV	107 ± 27 mL	107 ± 18 mL	0 ± 13 mL	0.51	0.92 (0.003)	−9–9 mL	13%
MV EPFR	579 ± 101 mL/sec^2	661 ± 115 ml/sec^2	−82 ± 150 mL/sec^2	0.17	0.06 (0.46)	−186–23 mL/sec^2	24%
MV APFR	268 ± 57 mL/sec^2	303 ± 62 mL/s^2	−35 ± 29 mL/sec^2	0.18	0.52 (0.15)	−80–11 mL/sec^2	23%
MV E/A	2.2 ± 0.4	2.3 ± 0.5	−0.1 ± 0.4	0.51	0.77 (0.04)	−0.4–0.2	19%

Abbreviations: SD, standard deviation; ICC, intraclass correlation coefficient; CI, confidence interval; COV, coefficient of variation; LVEDV, left ventricular end-diastolic volume; LVESV, left ventricular end-systolic volume; LV SV, left ventricular stroke volume; LV EF, left ventricular ejection fraction; LVEDM, left ventricular end-diastolic mass; MV SV, trans-mitral stroke volume; MV EPFR, trans-mitral early peak filling rate; MV APFR, trans-mitral atrial peak filling rate; MV E/A, ratio between trans-mitral EPFR and APFR.

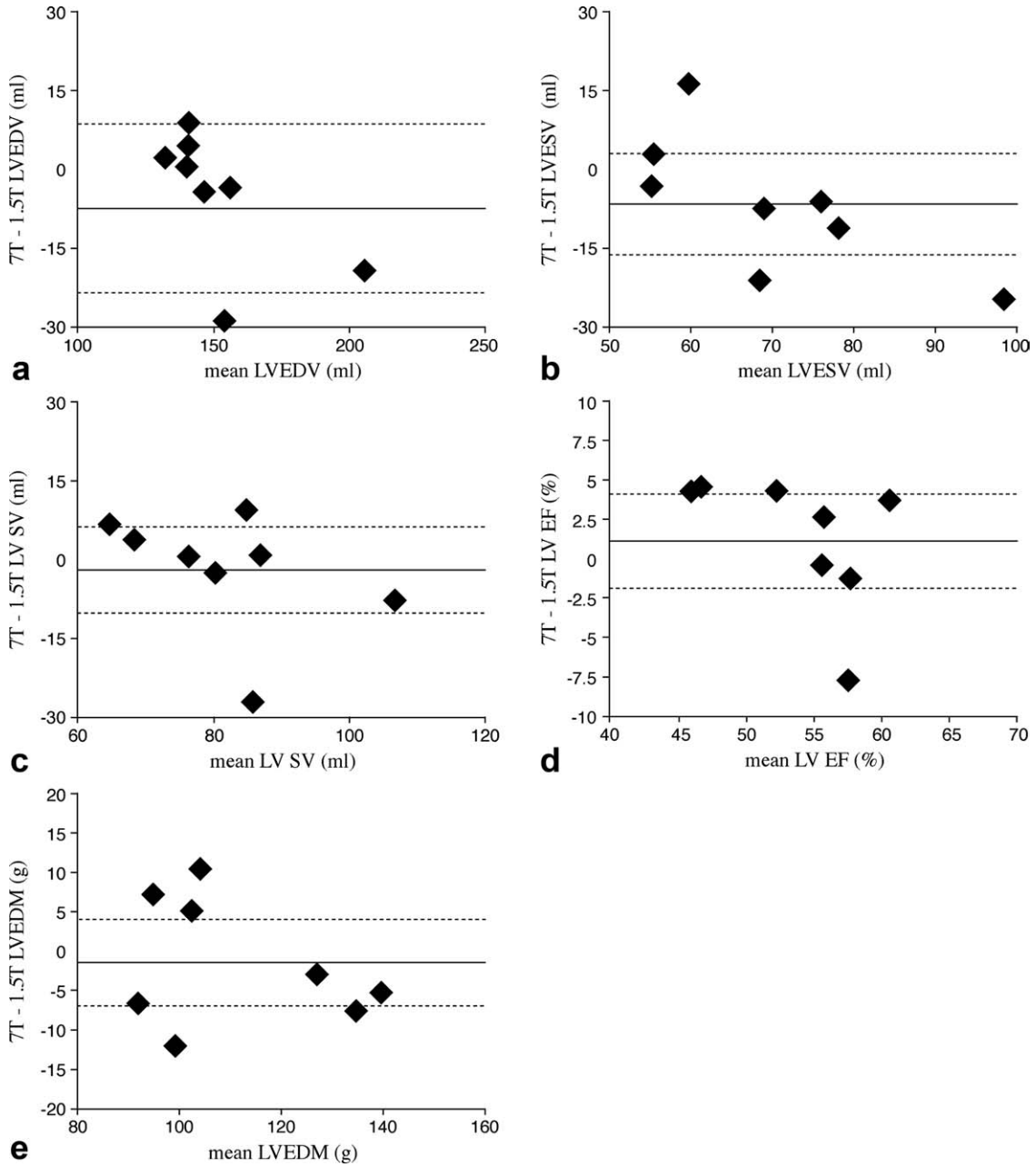

FIG. 2. Bland Altman-plots for LV volumes, function, and mass from short-axis assessment at 7 T MRI and 1.5T MRI. **a**: LVEDV left ventricular end-diastolic volume. **b**: LVESV left ventricular end-systolic volume. **c**: LVSV left ventricular stroke volume. **d**: LV EF left ventricular ejection fraction. **e**: LVEDM left ventricular end-diastolic mass. No obvious trends in bias are present.

differences in LV volumes, function, or mass obtained from short-axis data acquired at 7 T MRI and 1.5 T MRI. The variables assessed from short-axis scans at 7 T MRI agreed well with variables assessed at 1.5 T MRI (intraclass correlation coefficients between 0.77 and 0.92). The variation in left ventricular end-systolic volume was highest (19%), whereas left ventricular end-diastolic volume and LV stroke volume showed 14% variation and ejection fraction and mass only 8% and 7%. The Bland-Altman-plots are presented in Fig. 2. No obvious trends in bias were present.

Trans-Mitral Flow

Also in Table 1, results for comparison of trans-mitral stroke volume, early and atrial peak filling rate, and E/A-ratio are presented. No statistically significant difference between stroke volumes assessed with 7 T MRI and 1.5 T MRI was found, the correlation was strong, and the coefficient of variation was 13%. Assessment of early peak filling rate and atrial peak filling rate from the trans-mitral flow graphs showed more variation (up to 24%) between the two field strengths, correlation was moderate to poor, although differences were not

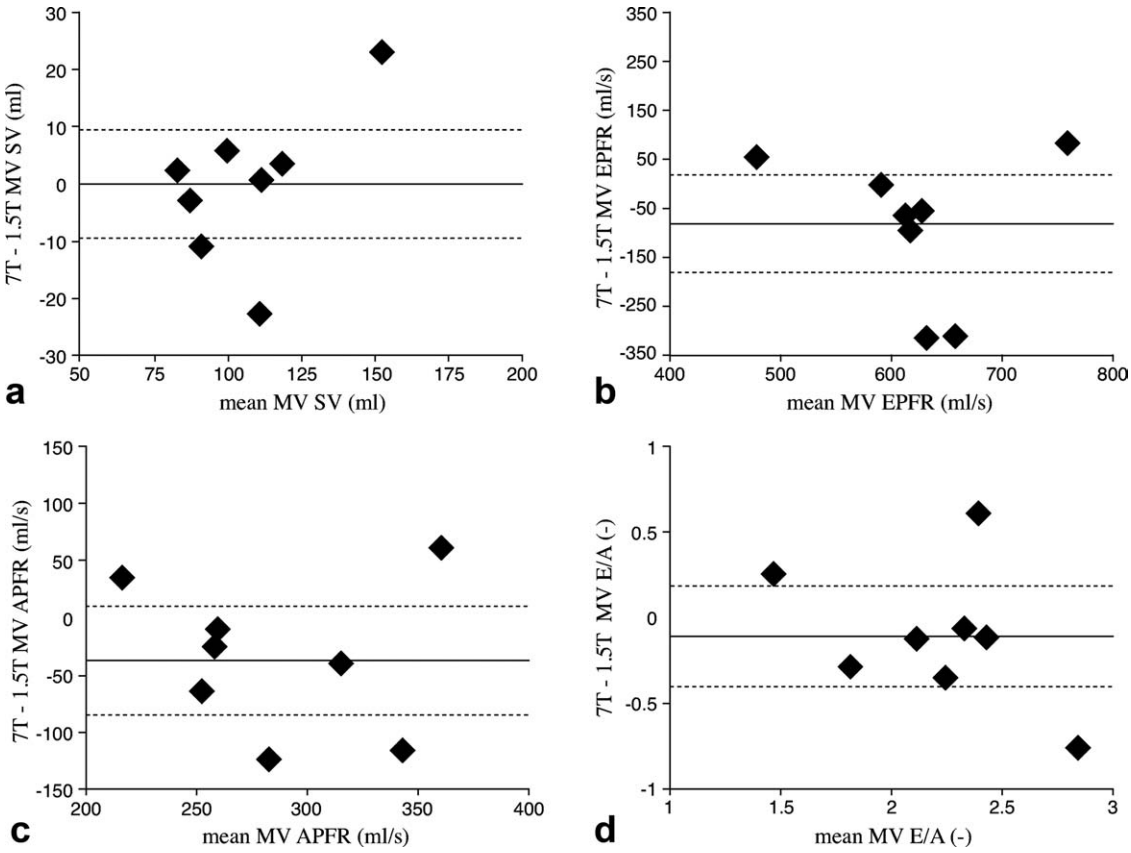

FIG. 3. Bland Altman-plots for trans-mitral flow assessment at 7 T MRI and 1.5 T MRI. **a**: MV SV: trans-mitral stroke volume. **b**: MV EPFR: trans-mitral early peak filling rate. **c**: MV APFR: trans-mitral atrial peak filling rate. **d**: MV E/A: ratio between trans-mitral EPFR and APFR. No obvious trends in bias are present.

statistically significant. Correlation for E/A-ratio was good (intraclass correlation coefficient 0.77). Bland-Altman-plots are presented in Fig. 3: no obvious trends in bias were present.

SNR and contrast-to-noise ratio

The results for SNR and contrast-to-noise ratio-measurements are presented in Table 2. The mean SNR measured in the LV blood pool was higher at 7 T MRI, but the difference with 1.5 T MRI was not statistically significant. The mean SNR measured in the interventricular septum was significantly higher at 7 T MRI versus 1.5 T MRI (roughly a factor-of-two), whereas in the LV lateral wall, SNR at 7 T MRI was significantly lower than at 1.5 T MRI (also roughly a factor-of-two). This demonstrates that the drop-off in SNR between the interventricular septum and LV lateral wall from the surface-coil transmit and receive profiles was approximately a factor-of-four, whereas the SNR for these two regions in the 1.5 T scans were the same, illustrating the more homogeneous distribution of signal in the 1.5 T MRI scans.

DISCUSSION

The main findings of this study are that the quantitative values of LV volumes, function, and mass at 7 T MRI agree well with the "gold standard" of 1.5 T MRI. In addition, assessment of trans-mitral stroke volume and ratio between early and atrial peak filling rates from VE MRI at 7 T MRI also show strong agreement with assessment at 1.5 T MRI, whereas the early and atrial peak filling rates, although statistically nonsignificantly different, display a greater variation at 7 T MRI versus 1.5 T MRI.

Comparison studies between 1.5 T MRI and 3 T MRI have already shown that an increase in field strength

Table 2
Comparison of SNR and CNR at 7 T MRI Versus 1.5 T MRI

	7 T MRI, mean ± SD	1.5 T MRI, mean ± SD	Mean difference ± SD	*P*-value
SNR interventricular septum	63 ± 23	36 ± 21	27 ± 31	0.04
SNR LV lateral wall	18 ± 5	36 ± 17	-18 ± 20	0.04
SNR LV blood pool	110 ± 32l	78 ± 47	32 ± 59	0.16
CNR blood pool-septum	47 ± 10	42 ± 26	5 ± 31	0.64
CNR blood pool-lateral wall	93 ± 29	42 ± 32	51 ± 42	0.01

Abbreviations: SNR, signal-to-noise ratio; CNR, contrast-to-noise ratio; SD, standard deviation.

does not warrant a straightforward increase in image quality (17–22). Technical difficulties limiting the full potential of high field scanning need to be overcome or at least to be taken into account when working at a human whole-body 7 T MRI system. The use of SSFP pulse sequences, providing excellent contrast between myocardium and blood at 1.5 T MRI and therefore, the method-of-choice for LV function and volume assessment, has not yet been demonstrated at 7 T MRI (and is even still very challenging at 3 T MRI) due to the presence of susceptibility artifacts, banding artifacts, and specific absorption rate constraints limiting the use of a short RF TR. Also, a transmit/receive coil is not commercially available for 7 T MRI scanning. We used an in-house constructed 13-cm-diameter quadrature double-loop RF transmit/receive surface coil operating at 298.1 MHz for the 7 T MRI examinations. With the current setup, the RF penetration depth was sufficient to visualize the posterior LV wall, therefore making LV segmentation possible. However, development of larger surface coils or coil arrays with elements positioned on the backside of the volunteer will improve RF penetration depth, potentially resulting in increased SNR in the posterior wall of the LV and more homogeneous distribution of signal intensity in the imaging plane and therefore, potentially resulting in a more reliable LV segmentation. SNR in the interventricular septum was higher at 7 T MRI when compared with 1.5 T MRI. The use of an SSFP-sequence in combination with the five-element phased-array surface receive coil and more robust cardiac triggering at 1.5 T MRI results in overall superior image quality with a more homogeneous distribution of signal when compared with the current implementation of cardiac acquisition schemes and parameters at 7 T MRI. Nevertheless, despite the inhomogeneous signal distribution at 7 T MRI, this did not lead to statistically significant differences in LV volumes, function, and mass at 7 T MRI versus 1.5 T MRI. The assessed variables also showed good agreement with 1.5 T MRI, illustrating that image quality for cine gradient-echo short-axis MRI at 7 T was adequate for reliable segmentation.

This study is the first to report intraventricular flow assessment by VE MRI at 7 T MRI and our results proved that trans-mitral flow assessment is feasible. Excellent agreement between 7 T MRI and 1.5 T MRI for mitral valvular stroke volume assessment was found. Also, assessing E/A-ratio did not show significant differences between MRI-acquisition at 7 T MRI and 1.5 T MRI. On the other hand, the poor agreement for assessing early and atrial peak filling rates at 7 T MRI and 1.5 T MRI illustrates that accurate depiction of the maxima in the trans-mitral flow graphs (i.e., the parameters describing diastolic filling) remains difficult due to the limited temporal resolution of the graphs (i.e., only 40 phases per cardiac cycle).

Local phase offset errors caused by concomitant gradients can significantly corrupt flow assessment with VE MRI (23). No background phase correction was performed as described by Chernobelsky et al. (14), but by using the method of local background correction (i.e., subtracting the mean velocity from nearby myocardium from the velocity through the mitral annulus), it can be assumed that besides correcting for through-plane motion, also local phase offset errors are eliminated.

Our study does have some limitations. Only 10 volunteers were included and 7 T MRI-acquisition was successful in 80% of these examinations, giving a group size of eight overall. Nevertheless, good agreement with 1.5 T MRI was found despite the small sample size. Interstudy reproducibility still needs to be assessed by studying subjects repeatedly. Furthermore, patients with variable severity of heart failure need to be evaluated to study the value and robustness of the technique in estimating the degree of LV dysfunction.

CONCLUSIONS

This study shows the feasibility of assessing LV volumes, function, and flow at 7 T MRI and demonstrated that the current acquisitions techniques at 7 T MRI provide similar quantitative results as compared to the gold standard of 1.5 T MRI. It is to be anticipated that further optimization of coil design (1,2,5,6) and acquisition schemes will continue to improve cardiac MRI technology at 7 T.

REFERENCES

1. Snyder CJ, DelaBarre L, Metzger GJ, van de Moortele PF, Akgun C, Ugurbil K, Vaughan JT. Initial results of cardiac imaging at 7 Tesla. Magn Reson Med 2009;61:517–524.
2. Vaughan JT, Snyder CJ, DelaBarre LJ, Bolan PJ, Tian J, Bolinger L, Adriany G, Andersen P, Strupp J, Ugurbil K. Whole-body imaging at 7T: preliminary results. Magn Reson Med 2009;61:244–248.
3. Van Elderen SGC, Versluis MJ, Webb AG, Westenberg JJM, Doornbos J, Smith NB, de Roos A, Stuber M. Initial results on in vivo human coronary MR angiography at 7 T. Magn Reson Med 2009;62: 1379–1384.
4. Frauenrath T, Hezel F, Heinrichs U, Kozerke S, Utting JF, Kob M, Butenweg C, Boesiger P, Niendorf T. Feasibility of cardiac gating free of interference with electro-magnetic fields at 1.5 Tesla, 3.0 Tesla and 7.0 Tesla using an MR-stethoscope. Invest Radiol 2009;44: 539–547.
5. Maderwald S, Orzada S, Schäfer LC, Bitz AK, Brote I, Kraff O, Theysohn JM, Ladd ME, Ladd SC, Quick HH. 7T Human in vivo cardiac imaging with an 8-channel transmit/receive array. In: Proceedings of the 17th Annual Meeting of ISMRM, Honolulu, HI, USA, April 18–24, 2009 (Abstract 821).
6. Frauenrath T, Renz W, Patel N, Hezel F, Dieringer M, Schulz-Menger J, Niendorf T. Cardiac imaging at 7.0 T: comparison of pulse oximetry, electrocardiogram and phonocardiogram triggered 2D-CINE for LV-function assessment. In: Abstracts of the 13th Annual SCMR Scientific Sessions, Phoenix, Arizona, USA, January 21–24, 2010, J Cardiovasc Magn Reson 2010;12 Suppl 1:O15.
7. Fischer SE, Wickline SA, Lorenz CH. Novel real-time R-wave detection algorithm based on the vectorcardiogram for accurate gated magnetic resonance acquisitions. Magn Reson Med 1999;42:361–370.
8. Perman WH, Bernstein MA, Sandstrom JC. A method for correctly setting the RF flip angle. Magn Reson Med 1989;9:16–24.
9. Versluis MJ, Tsekos N, Smith NB, Webb AG. Simple RF design for human functional and morphological cardiac imaging at 7 Tesla. J Magn Reson 2009;200:161–166.
10. Suits BH, Garroway AN, Miller JB. Surface and gradiometer coils near a conducting body: the lift-off effect. J Magn Reson 1998;135: 373–379.
11. van der Geest RJ, de Roos A, van der Wall EE, Reiber JHC. Quantitative analysis of cardiovascular MR images. Int J Card Imaging 1997; 13:247–258.
12. van der Geest RJ, Reiber JHC. Quantification in cardiac MRI. J Magn Reson Imaging 1999;10:602–608.
13. van der Geest RJ, Niezen RA, van der Wall EE, de Roos A, Reiber JHC. Automated measurement of volume flow in the ascending aorta using MR velocity maps: evaluation of inter- and intraobserver

variability in healthy volunteers. J Comput Assist Tomogr 1998;22: 904–911.
14. Chernobelsky A, Shubayev O, Comeau CR, Wolff SD. Baseline correction of phase contrast images improves quantification of blood flow in the great vessels. J Cardiovasc Magn Reson 2007;9:681–685.
15. Kayser HWM, Stoel BC, van der Wall EE, van der Geest RJ, de Roos A. MR velocity mapping of tricuspid flow: correction for through-plane motion. J Magn Reson Imaging 1997;7:669–673.
16. Bland JM, Altman DG. Statistical methods for assessing agreement between two methods of clinical measurement. Lancet 1986;8:307–310.
17. Noeske R, Seifert F, Rhein KH, Rinneberg H. Human cardiac imaging at 3 T using phased array coils. Magn Reson Med 2000;44:978–982.
18. Hinton DP, Wald LL, Pitts J, Schmitt F. Comparsion of cardiac MRI on 1.5 and 3.0 Tesla clinical whole body systems. Invest Radiol 2003;38:436–442.
19. Greenman RL, Shirosky JE, Mulkern RV, Rofsky NM. Double inversion black-blood fast spin-echo imaging of the human heart: a comparison between 1.5 T and 3.0 T. J Magn Reson Imaging 2003;17: 648–655.
20. Bi X, Deshpande V, Simonetti O, Laub G, Li D. Three-dimensional breathhold SSFP coronary MRA: a comparison between 1.5 T and 3.0 T. J Magn Reson Imaging 2005;22:206–212.
21. Hudsmith LE, Petersen SE, Tyler DJ, Francis JM, Cheng ASH, Clarke K, Selvanayagam JB, Robson MD, Neubauer S. Determination of cardiac volumes and mass with FLASH and SSFP cine sequences at 1.5 vs. 3 Tesla: a validation study. J Magn Reson Imaging 2006;24: 312–318.
22. Liu X, Bi X, Huang J, Jerecic R, Carr J, Li D. Contrast-enhanced whole-heart coronary magnetic resonance angiography at 3.0 T: comparison with steady-state free precession technique at 1.5 T. Invest Radiol 2008;43:663–668.
23. Kilner PJ, Gatehouse PD, Firmin DN. Flow measurement by magnetic resonance: a unique asset worth optimising. J Cardiovasc Magn Reson 2007;9:723–728.